ISSN: 2447-3359

REVISTA DE GEOCIÊNCIAS DO NORDESTE

Northeast Geosciences Journal

v. 11, nº 2 (2025)

https://doi.org/10.21680/2447-3359.2025v11n2ID40548

Heat islands on urban surfaces in the Brazilian Midwest: a case study

Ilhas de calor em superfícies urbanas no Centro-Oeste brasileiro: um estudo de caso

Estéfane da Silva Lopes[1]; Karla Emmanuela Ribeiro Hora[2]

[1] Federal Institute of Tocantins, Palmas Campus, Palmas/TO, Brazill. Email: estefane_lopes@hotmail.com
ORCID: https://orcid.org/0000-0002-1527-2960

[2] Federal University of Goiás, Goiânia Campus, Goiânia/GO, Brazil. Email: karla_hora@ufg.br
ORCID: https://orcid.org/0000-0002-4410-3728

Abstract: Permeability represents the ability of water to infiltrate the soil surface. On urban surfaces such as paved streets, buildings on impermeable soils, which are resistant to permeability and infiltration, lead to different impacts on the environment, including the phenomenon of heat islands. This phenomenon is characterized by an increase in temperature in urban centers compared to their surroundings. Therefore, this study aims to investigate the impact of permeability on the formation of heat islands in an area of a neighborhood located in the city of Goiânia, Goiás, Brazil. To this end, the intensity of the heat island was verified through on-site measurements located in the densest and most vertical neighborhood in Goiânia, the Bueno Sector. Based on these measurements, the permeability and surface temperature around the collection points were mapped using a Landsat-08 image. The results of the measurements showed that heat island formations are usually more intense in the early hours of the morning (at night), reaching an amplitude of up to 10° C (heat island of very strong magnitude). The results show a correlation between the formation of urban heat islands and the typologies of urban land use and occupation, highlighting: urban densification and impermeability for the locations with the highest occurrences of urban heat islands.

Keywords: Urban heat islands; Urban Permeability; Goiânia.

Resumo: A permeabilidade representa a capacidade de a água infiltrar-se na superfície do solo. Em superfícies urbanas como ruas asfaltadas e edificações sobre solos impermeáveis, a resistência à permeabilidade e à infiltração leva a impactos distintos sobre o ambiente, dentre os quais está o fenômeno de ilhas de calor. Tal fenômeno caracteriza-se pelo aumento da temperatura nos centros urbanos em comparação aos do entorno. Sendo assim, este trabalho teve como objetivo investigar o impacto da permeabilidade na formação de ilhas de calor em uma área de um bairro localizado na cidade de Goiânia, Goiás, Brasil. Para tanto, verificou-se a intensidade da ilha de calor por meio de medições in loco realizadas no bairro mais adensado e verticalizado de Goiânia, o Setor Bueno. A partir dessas medições, realizou-se o mapeamento da permeabilidade e da temperatura superficial no entorno dos pontos de coleta, com o uso de imagem do Landsat-08. Os resultados das medições permitiram verificar que, geralmente, as ilhas de calor são mais intensas à noite e nas madrugadas, atingindo amplitude de até 10°C (ilha de calor de magnitude muito forte). Os resultados evidenciam a correlação entre a formação das ilhas de calor urbanas e as tipologias de uso e ocupação do solo urbano, destacando o adensamento urbano e a impermeabilidade nas localidades com maiores ocorrências do fenômeno.

Palavras-chave: Ilhas de Calor Urbanas; Permeabilidade; Goiânia.

Received: 18/06/2025; Accepted: 24/10/2025; Published: 04/12/2025.

1. Introduction

The city is a very ancient organization, marking its presence in history through elements that signal the advent of what is considered civilization. Economic and social processes are outlined, transforming living conditions: population concentrations, rural migrations, overpopulation, and space transformation mark the growth and configuration of cities (PESAVENTO, 1995).

From the formation of cities to the growth of urban agglomerations, numerous and distinct processes have been observed, whose basis of economic and technological transformation was anchored in socio-spatial inequalities with repercussions on nature. However, the development model occurred in a disorderly manner, and often these inequalities revealed a lack of environmental concerns and universal access to basic infrastructure. Consequently, the city and its urban nuclei, in particular, began to experience structural problems that harm environmental quality of life.

Thus, urbanization has transformed cities into densified areas with less vegetation and a greater quantity of various artificial surfaces. Consequently, the loss of vegetation increases heat storage in the soil layer, which, in turn, contributes to the rise in air temperature in urban areas (OKE, 1987).

Estimating that more than 68% of the world's population will live in urban areas by 2050 (UN, 2018), it must be considered that the ongoing urbanization pattern will accentuate the problems already occurring in cities, impacting the majority of human beings. Among these problems, the alteration of urban climate has been a constant concern in various studies (CHEN et al. 2006; NASCIMENTO, 2011). Nakata-Osaki et al. (2018) state that population growth in urban areas drives urban climate studies for two important reasons: to verify the effects of urbanization on climate and to ensure a pleasant and healthy environment for the urban population.

Given the increase in temperature in cities, it is important for planners to consider adverse health effects such as respiratory problems due to increased ozone levels, thermal stress, and heat-induced mortality in their planning strategies.

Thus, it is increasingly necessary for urban climate studies to understand how the increase in this dense constructive gradient (buildings, streets, infrastructure works, etc.) affects the environment.

According to Dorigon and Amorim (2019), aspects related to roughness, vegetation, and urban densification, combined with others of an economic and social nature, can be determinant for the analysis of urban climate, as they allow and intensify the energy exchange between the surface and the atmosphere.

According to Oke (1981), low permeability caused by the use of paving, which has replaced natural cover, leads to a decrease in green areas, thus modifying the thermal energy balance and consequently altering the thermal exchanges between surfaces and the environment. In this context, vegetation aims to reduce environmental extremes, as it tends to stabilize air temperature and filter atmospheric pollutants, in addition to providing better urban ventilation (DUARTE, 2002).

Since the topic has received greater attention since the last years of the 20th century, the phenomenon of urban heat islands (UHI), according to Iping et al. (2019), can be defined as the observed difference in ambient temperature between central urban areas and peripheral ones.

For Oke (1987), urban heat islands originate mainly from the urban development model, not committed to planning, which results in higher land surface temperature, since the characteristics of construction materials and urban geometry lead to heat retention, something that can be observed through remote sensing data and not just meteorological data. However, studies on urban heat islands not only help to perceive long-term urban environment changes but also to propose improvements for the quality of life in a given region (CHEN et al. 2020).

Various researches, such as those by Deng et al. (2009); Hu and Brunsell, (2013); Budhiraja, Pathak and Agrawal, (2017); Dorigon and Amorim, (2019); Wang et al. (2019), present the effects caused by urban heat islands around the world.

It should be emphasized that knowing the magnitude and impact of urban heat islands in a given location is important for defining guidelines for efficient and sustainable urban planning, thus working for the well-being of the population residing in the city.

In the United States, there is a concern among states and municipalities, and many local governments are increasingly interested in protecting and preparing people for the urban heat island phenomenon, applying environmental control principles to mitigate them (EPA, 2020).

In Brazil, the importance of studies of this nature is also latent. As the country has few studies on urban heat islands (DORIGON AND AMORIM, 2019), it becomes relevant to deepen studies of this nature to broaden the understanding of this phenomenon in different Brazilian cities and regions, so that their results can be used by public authorities.

In Goiânia, the problem related to urban heat islands is smaller compared to large cities undergoing a process of accelerated economic and industrial growth. However, disordered urban occupation, combined with a lack of planning, means that the city also presents urban environmental problems.

Among the factors affecting the intensity of the urban heat island phenomenon, Rajagopalan et al. (2014) classify them into two groups: the first involves meteorological aspects such as wind speed and direction, humidity, and cloud cover; and the second group refers to factors related to city design such as density of built areas, paving, and vegetation cover.

Luan et al. (2020) state that the absence of vegetation cover is the most important determinant for the formation of urban heat islands, and anthropogenic actions are gaining prominence increasingly on a global scale, acting in the suppression of vegetation. Furthermore, according to the authors, given the complexity and importance of studies on urban surfaces and their impact on the formation of the urban heat island phenomenon, a deeper analysis of the most densified and verticalized neighborhoods regarding the formation of the phenomenon becomes necessary, proposing the inclusion of new parameters and highlighting the advantages of using remote sensing for the study.

Considering that urban heat islands are more likely to occur in areas of greater urban densification, with a higher concentration of buildings, soil impermeabilization, and less vegetation cover, the research main objective was to investigate the impact of the permeability of horizontal urban surfaces on the formation of urban heat islands in the Bueno Sector, located in the city of Goiânia, Goiás, Brazil.

2. Methodology

2.1. Research Design

The research is a case study that confronted the conditions of urban permeability and the occurrence of heat islands in an area of the Bueno sector in Goiânia-GO with in loco data collection, through measurements carried out at specific points. For this purpose, an area of the Setor Bueno neighborhood was chosen, as it is the neighborhood in Goiânia with the greatest urban densification and consequent surface impermeabilization. Once the study area in the neighborhood was defined, the definition of measurement points, equipment used, measurement period, survey of permeability at the measurement points, and elaboration of urban permeability maps were carried out.

2.2. Choice and Characterization of the Study Area

For the study, an area of the Setor Bueno neighborhood located in the city of Goiânia, Goiás, Brazil, was chosen. This area has greater verticalization and densification compared to the rest of the neighborhood. For a better understanding of the analyses to be addressed, it was necessary to describe the city according to its geographical, climatic, and urbanistic characteristics.

The city of Goiânia is located in the South-Central region of the state of Goiás, between the latitude of 16° 40' 48" South and longitude 49° 15' 18" West, with an approximate area of 729 km² (IBGE, 2010).

According to the Brazilian Institute of Geography and Statistics (IBGE), Goiânia has a predominantly urban population estimated at around 1,536,097 people in the year 2020 (IBGE, 2020).

The urban growth of the municipality, considering its origin in 1936 to the present moment, is characterized by an intense migratory process, mainly in the 1960s, with the construction of Brasília, and in the 1980s, with the modernization of agriculture, which brought a large number of people from the interior of the state to the city (SOUSA; FERREIRA, 2019).

The climate of Goiânia can be classified by the regional air circulation systems that act in the Midwest region, by its latitudinal position, and by the lack of water bodies, contributing to a hot and rainy summer, a spring with the highest temperatures of the year, and a dry winter with high thermal amplitude (NASCIMENTO; BARROS, 2009). It is possible to characterize it based on climatological normals (meteorological data obtained by INMET). According to Oke (1987) and the Köppen climate classification, Goiânia falls under the tropical type (Aw) – Tropical Climate with a dry season in winter and rains in summer.

Regarding precipitation in Goiânia, it can be concluded that rains occur more frequently from November to March, and the driest months correspond to June to August, with low occurrences of precipitation.

According to Nascimento (2011), the hottest months are more humid and the coldest are drier. There is a probable relationship between the temperature increase and anthropogenic actions related to forms of use and occupation of the urban territory, influencing the microclimate of Goiânia.

However, the microclimate of Goiânia undergoes global and local changes, but anthropogenic actions, at the local scale of the city, influence it positively and/or negatively. This is why we are interested in quantifying and qualifying this interference.

The study was based on a neighborhood in Goiânia and the selection criteria used were: the most populous and densified neighborhoods according to data from the city hall in 2013. The verticalization that each region is currently undergoing was also analyzed, through the analysis of data provided by the Association of Companies in the Real Estate Market of Goiás. Figure 1 shows the urban densification of Goiânia by neighborhood.

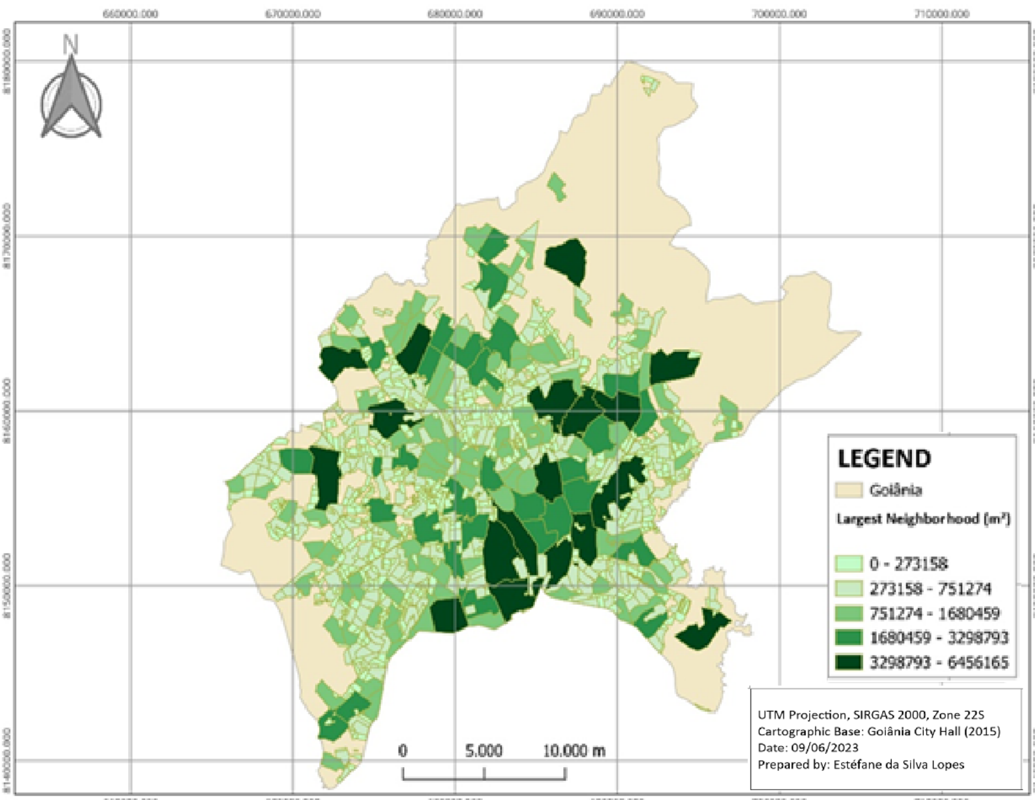

Figure 1 – Urban Densification of Neighborhoods in the Region of Goiânia.
Source: Authors (2023).

The number of vertical buildings by neighborhoods in the Southern Sector was also verified, with the respective number of floors (Figure 2).

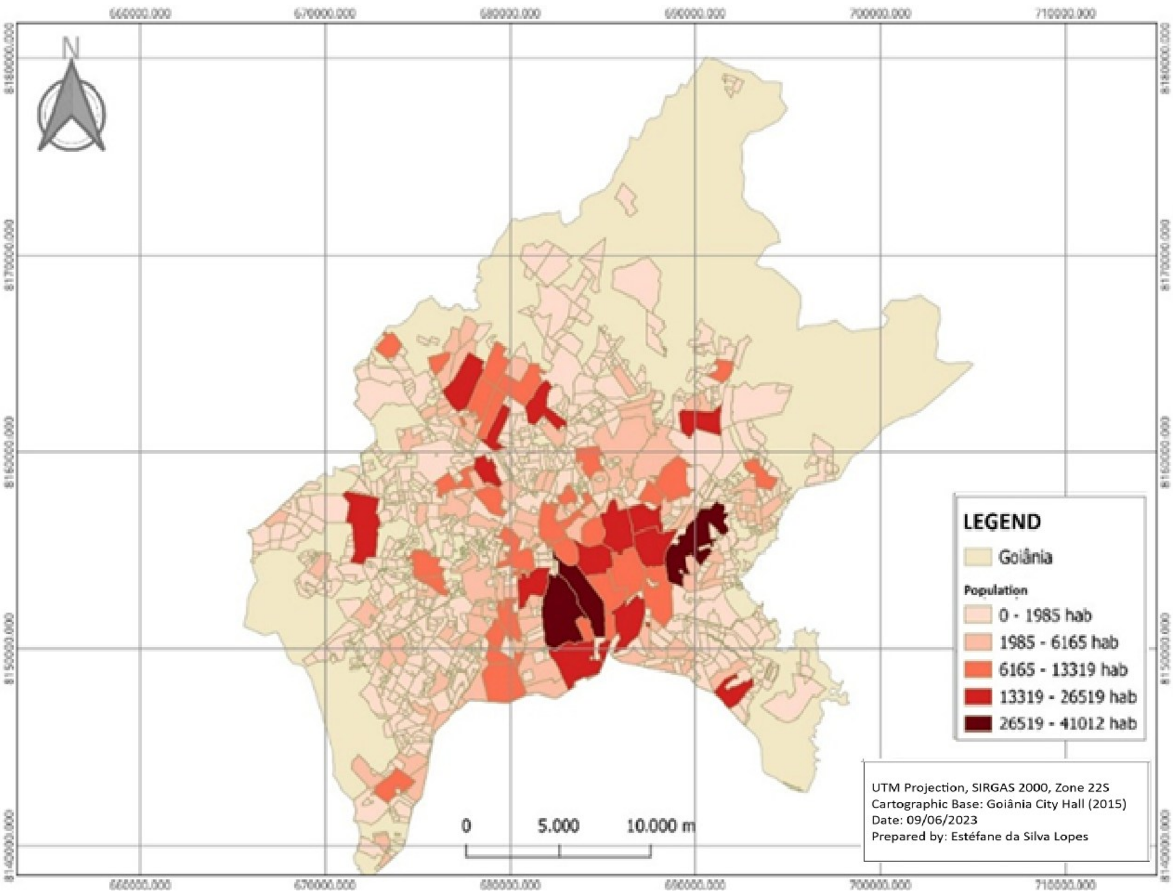

Figure 2 – Distribution of Vertical Buildings by Neighborhoods in Goiânia.
Source: Authors (2023).

As it has the highest population density among the neighborhoods in the southern region, the Setor Bueno neighborhood was chosen. This neighborhood has the highest number of launched buildings, the highest number of constructed buildings, and the highest concentration of buildings above 30 floors.

Setor Bueno is the neighborhood of Goiânia, located in the Southern region, as shown in Figure 1, which presents the administrative regions and verticalization of Goiânia. The neighborhood has higher population density, a higher number of buildings under launch, and a higher number of taller buildings, in addition to having a predominant vertical typology.

Once the more intense verticalization of the city's Southern region was verified, it was decided to detail it, highlighting the area and population of each neighborhood that composes the region (Figure 3).

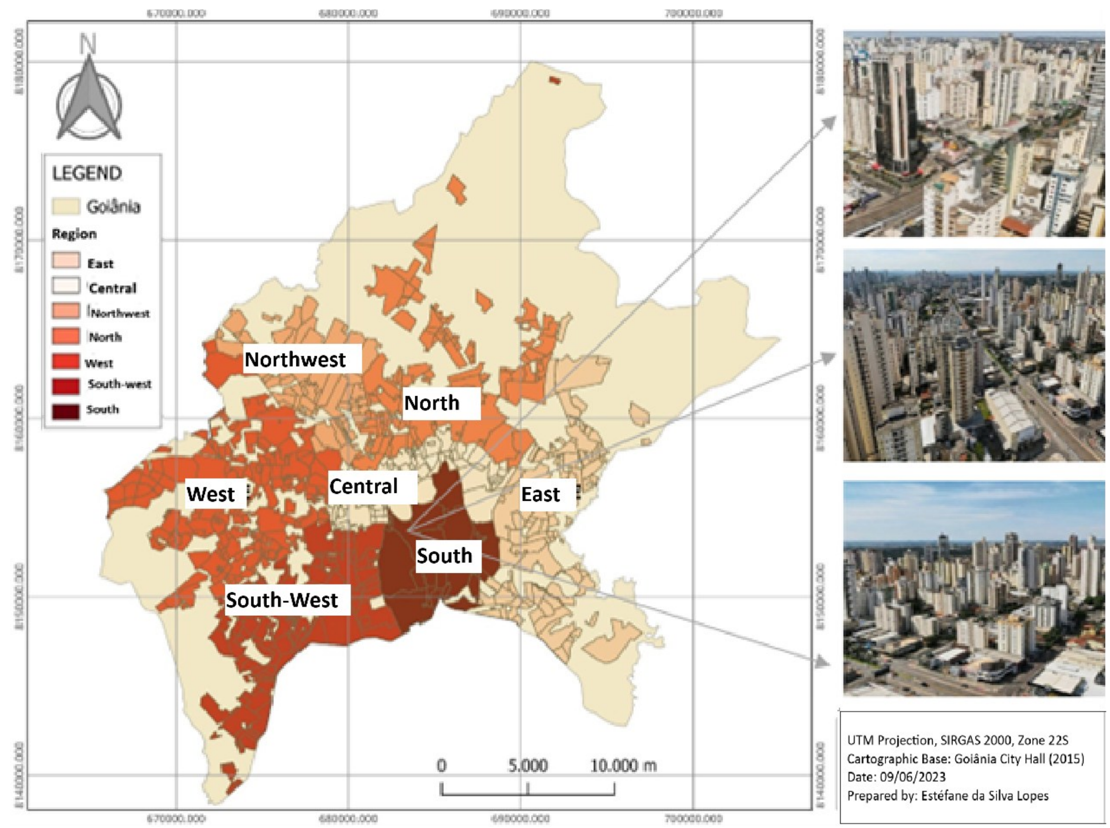

Figure 3 – Administrative Regions of Goiânia and Verticalization in the Bueno Sector (Southern Region). Source: Authors (2023).

This work initially proposed the mapping and analysis of census data (from IBGE and the Goiânia city hall), in which several neighborhoods were considered and evaluated. Figure 4 presents the location map of the studied area.

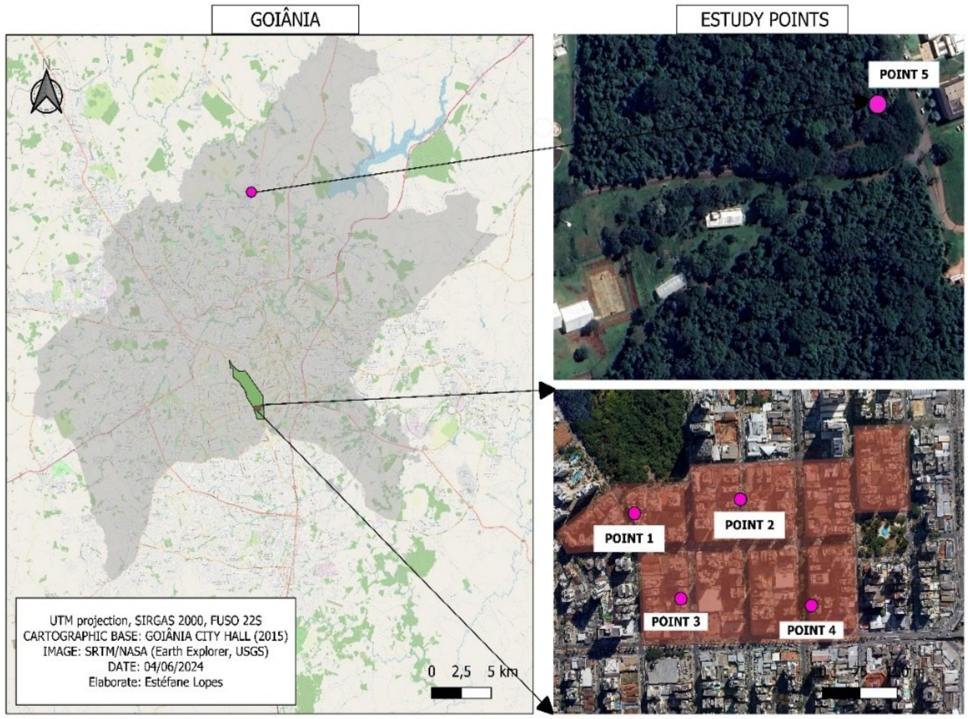

Figure 4 – Location Map of the Study Area.
Source: Authors (2023).

It was found that the blocks with the tallest buildings (above 30 floors) in the neighborhood were located in the study area, facing the neighborhood's largest park, the Vaca Brava Park.

2.3. Definition of Measurement Points

A second stage of the work was the measurement of air temperatures. For this, measurement points were selected. The criterion for choosing the points was the variety of the type of urban occupation. However, the number of collection points was limited by the availability of equipment, in addition to the difficulty in installing the equipment safely and leaving it for the necessary period of time. Given these conditions, the collection was done at 5 points, with P1, P2, P3, and P4 being urban and P5 rural, in a verticalized area of Setor Bueno. Among the 5 points, for standardization, 3 urban points were installed at a height of 1.50m from the surface, tied to a tree in front of the vertical buildings, and one point in a vehicle parking lot. The rural point was installed in the woodland located at the Federal University of Goiás, in front of the FAV building – Faculty of Visual Arts. This procedure allowed establishing the hourly temperature differences between the reference points in the urban area and the rural area. Table 1 presents details on the installation of the equipment**.**

Table 1 – Locations of Meter Installation.

Point	Altitude	Coordinates		Address
		Longitude (E)	Latitude (S)	
1	815m	684393.28m	8151540.32m	T15 Avenue corner of T66, Setor Bueno
2	820m	684650.67m	8151591.84m	T38 Avenue corner of R.T61, Setor Bueno
3	824m	684522.90m	8151334.13m	Avenue.T5, Setor Bueno
4	830m	684785.68m	8151354.15m	Avenue.T4, Setor Bueno
5	785m	685283.03m	8163233.81m	R.do Bosque, Samambaia Campus

Fonte: Authors (2023).

Figure 4 shows the detailed location of the measurements.

Vegetation predominates around Point 1, located near a park and a lake in a predominantly residential area consisting only of tall buildings. Point 1 is located in Section A.

Point 2 is located near a shopping mall, in a parking lot. The area features a mix of commercial and residential use with tall buildings. The equipment was installed in Section C.

Point 3 is located in a mixed-use area: commercial and residential, fully verticalized with buildings. P3 is located in Section J. The street provides access to the neighborhood's park and lake.

Point 4 is located in a predominantly commercial mixed-use area, near tall buildings, with tree vegetation between the roadway. P4 is located in Section L.

Point 5 was installed in the vicinity of a dense forest located on the Samambaia campus, covered in tree vegetation and home to endangered animal species.

Figure 4 – Detailing of the Surroundings of the Measurement Locations at the 5 Points.
Source: Authors (2023).

2.4. Measurement Periods

To meet the research objective, the variables recorded during the measurements were air temperature and relative humidity. Basically, the analysis was done only in winter, especially in the transition to spring, a period in which there is high thermal amplitude. Three sets of measurements were carried out during the year 2021, according to (Table 2). The duration of the monitoring was 7 to 8 consecutive days, with a recording interval of 15 minutes.

Table 2 – Measurement Periods of Climate Variables.

Station	***Measurement period***	***Measurement range***	***Total***
Autumn/Winter	From June 18, 2021 to June 25, 2021	Every 15 minutes	7 days
Winter	From August 20, 2021 to August 27, 2021	Every 15 minutes	7 days
Winter	From September 8, 2021 to September 16, 2021	Every 15 minutes	7 days

Source: Authors (2023).

As the monitoring was done in two different seasons, a direct comparison was made between the average values of temperature and relative humidity of the air between the rural point P5 and all the remaining points.

Days with clear skies and low cloud cover were considered for the measurement days. The data were inserted into a spreadsheet and the simple statistical parameters of mean, maximum, and minimum temperature differences occurring between each urban point and the rural one were determined.

The data obtained in loco were based on an automatic station from the National Institute of Meteorology (INMET) and analyzed by cross-referencing urban permeability data from each point, in order to provide data suitable for the urban reality of Goiânia, thus allowing a better analysis of the space and contributing to a possible analysis of the urban problem and its diagnosis.

2.5. Equipament Used

According to Oke (2000), it is recommended for air temperature measurement that equipment be installed at a height between 1.25 to 2 meters in non-urban areas and in urban areas up to 5 meters above the ground.

5 distinct points were collected for recording air temperatures. At each point, RC-51H model dataloggers were installed, with an accuracy of +/- 0.3°C (for high resolution) and response time for still air programmed for 15 minutes simultaneously for each point. For uniformity, all points were installed at 1.5 meters above the ground, with their horizontal surfaces facing south and protected from direct solar radiation by means of protection devices specifically made for this purpose, in order to prevent the confinement of still air and allow natural ventilation of the sensors. An attempt was made to standardize the points in safe locations, avoiding proximity to certain materials.

A multifunctional device, available at the Laboratory of Environmental Monitoring Studies - LEMA of the School of Civil and Environmental Engineering - EECA of the Federal University of Goiás – UFG, was used to capture wind speed. Figure 5 shows the equipment used.

Multifunctional ***Datallogers (RC-51H)***

Figure 5 – Equipment Used for Manual and Automatic Measurement.
Source: Authors (2023).

Shelters made of rigid PVC in the horizontal direction were manufactured, the same as used by Valin Jr et al. (2016), as shown in Figure 6.

Point 1 Point 2 Point 3 Point 4 Point 5

Figure 6 – Equipment Installation Locations.
Source: Authors (2023).

The shelter was produced with rigid PVC tubes, white in color, requiring 0.6m in length with a diameter of 100mm and 0.5m in length with a diameter of 75mm. The smaller tube was coated on its external face with aluminum foil, to protect against possible thermal radiation effects. To center the smaller tube inside the larger tube, screws were used, allowing the datalogger and sensor to be centered, with ventilation and protected from weather conditions (Valin Jr et al., 2016).

According to the authors, the alternative model produced with rigid PVC tubes showed completely favorable results in all scenarios and analyses performed for fixed points.

2.6. Survey of Permeability at Measurement Points and Elaboration of Urban Permeability Maps

All urban points are located in regions of high verticalization. To quantify the respective percentages of soil permeability and impermeability, an influence radius was adopted as the area of influence. According to Oke (2006), the ratio between the height of the equipment and the radius of the area of influence for urban areas is 1:100. Considering that the height of the equipment used was 1.5m, a radius of 150m was adopted. The quantification was done from satellite images by automatic classification and by the AutoCAD program, using the land use map. The classification was checked with field data in order to eliminate possible errors.

2.7. Calculation of Urban Heat Island Intensity

Once the data were collected, data processing began. As the equipment recorded temperature and humidity measurements every 15 minutes (4 readings per hour), the average and maximum value for each hour of each measurement period was obtained.

From these values, the hourly subtraction between the temperatures of the urban points (P1 to P4) and the rural temperature (P5) occurred, thus obtaining the Urban Heat Island Intensity for each of the 4 urban points.

Once the hourly heat island value for each of the three periods was obtained, the intensity of the phenomenon throughout the periods was analyzed.

3. Results and discussion

3.1. Heat Island Intensity

Once the method was defined, data collection began. This collection occurred in three periods: 18/06 to 26/06 (period 01); 19/08 to 31/08 (period 02); and 08/09 to 16/09 (period 03).

It can be observed that the highest averages are presented in the third period, at around 30°C. The average value between the hottest and coldest month reaches 6°C, corroborating what is already expected in these months in Goiânia.

Once the temperatures were obtained, the urban heat island (UHI) intensity was calculated. For this, the temperatures of the points in the sector under study were subtracted from the temperature of the rural point located at the Samambaia Campus, as detailed earlier. Figures 5 to 9 present, respectively, the heat island intensity for points 1, 2, 3, and 4.

In general, it can be observed that the highest UHI values were found in period 01, with an hourly average of 3.13 °C. In turn, the period with the lowest daily average was period 02, with an average of 1.52 °C. It should be noted that, due to equipment problems, Point 03 did not show readings from 27/08 onwards in period 02 and did not show any readings in period 03.

It is observed that the heat island phenomenon occurs at night and especially in the early morning hours. The only exception was at point 02 in measurement period 01. In this situation, it was observed that even though heating is noted at night, the highest observed UHI values occurred between 09:00-12:00. As this only occurred in this season (winter) and at point P2, which is a parking lot, it is believed to be due to the temperature increase caused by its construction material.

Point P1 showed the lowest UHI intensity during the three periods (UHI= 1.8 ºC). Like the other points, the maximum UHI values occurred in (period P1), with averages between August and September being very close (around 1.3 ºC).

Point P2 showed the highest UHI among all points (2.7ºC) and the highest maximum UHI among the 4 points (10.4 ºC). This behavior is justified by the construction material of the thermometer installation site. Even close to the park, the type of construction material caused higher temperatures at the location.

Data	0:00	01:00	02:00	03:00	04:00	05:00	06:00	07:00	08:00	09:00	10:00	11:00	12:00	13:00	14:00	15:00	16:00	17:00	18:00	19:00	20:00	21:00	22:00	23:00	Total
18/06/2021																	1,7	3,1	3,7	3,6	4,6	5,4	5,1	4,8	4,0
19/06/2021	4,7	5,2	5,2	5,2	4,8	5,3	5,7	5,7	3,3	1,0	0,0	0,5	-0,5	-0,3	0,0	0,7	1,5	2,0	2,7	2,9	3,2	3,8	4,2	4,5	3,0
20/06/2021	4,1	4,1	4,2	4,0	3,9	3,8	3,8	3,8	3,6	3,5	2,0	2,1	0,8	0,0	0,4	1,9	1,5	2,0	2,7	2,5	3,2	3,4	3,6	3,5	2,8
21/06/2021	3,4	3,3	3,2	4,0	4,5	4,2	4,7	4,5	4,2	2,4	0,8	0,9	-0,8	-1,5	-1,2	-0,7	-8,6	-6,4	-3,1	-0,8	0,6	2,2	3,4	3,3	1,1
22/06/2021	3,8	5,2	5,1	5,4	5,0	4,3	4,3	4,2	3,6	3,3	0,7	-0,2	-0,9	-2,2	-2,1	-0,8	0,5	0,5	2,6	2,4	2,8	4,2	4,6	5,0	2,6
23/06/2021	5,2	5,0	5,4	5,4	5,2	5,1	5,4	5,5	3,3	1,6	-0,3	-0,5	-1,2	-1,7	-1,4	-0,9	0,0	2,0	3,8	4,3	4,3	4,6	5,1	4,9	2,9
24/06/2021	5,0	4,7	4,7	4,9	5,0	4,1	4,4	4,2	1,4	0,4	-0,2	0,7	-0,3	-0,6	-0,1	0,4	1,1	1,7	2,3	3,0	4,1	4,8	4,3	4,8	2,7
25/06/2021	5,6	5,6	5,2	5,0	4,5	4,4	4,4	4,2	3,4	1,9	0,0	0,2	-0,2	-0,9	-0,6	0,5	-0,1	2,4	4,1	3,9	3,8	3,9	3,8	3,7	2,9
26/06/2021	3,5	3,8	3,8	4,8	4,2	4,2	4,3	4,2	2,1	0,6	0,0	0,3	-0,4	-1,3	-1,1	-0,9	-0,5	-0,8	-0,4	0,0	-0,1				1,5
Total	4,4	4,6	4,6	4,8	4,6	4,4	4,6	4,5	3,1	1,8	0,4	0,5	-0,4	-1,1	-0,8	0,0	-0,3	0,7	2,0	2,4	3,0	4,0	4,3	4,3	2,5

Data	0:00	01:00	02:00	03:00	04:00	05:00	06:00	07:00	08:00	09:00	10:00	11:00	12:00	13:00	14:00	15:00	16:00	17:00	18:00	19:00	20:00	21:00	22:00	23:00	Total
20/08/2021																	0,4	-0,5	-0,7	2,4	1,7	1,8	3,0	2,1	1,3
21/08/2021	4,0	4,1	4,1	4,2	4,3	4,6	4,6	3,0	0,4	-1,8	-1,9	-1,5	-1,9	0,1	2,7	1,0	-0,4	-0,7	1,1	2,7	3,4	4,0	2,7	3,6	1,9
22/08/2021	4,0	4,0	4,3	4,5	4,2	3,0	3,1	1,8	-0,3	-1,4	-2,0	-2,0	-2,0	0,0	3,0	1,6	0,5	1,1	2,4	3,0	3,5	4,4	4,4	4,5	2,1
23/08/2021	3,9	4,1	4,2	4,9	5,3	5,5	5,1	3,7	1,1	-1,1	-2,1	-2,2	-2,1	0,3	2,0	1,0	-0,5	1,3	2,7	3,6	4,1	4,2	4,2	4,2	2,4
24/08/2021	4,1	4,0	3,4	3,2	2,9	4,0	4,5	3,9	1,3	-0,8	-2,0	-2,1	-2,3	-1,2	1,9	0,4	-0,8	0,6	2,3	3,3	3,4	3,5	4,0	4,7	1,9
25/08/2021	4,7	4,8	4,8	5,2	5,3	4,9	5,2	4,6	0,9	-1,1	-2,3	-2,2	-1,8	1,0	2,2	0,2	1,0	1,6	2,7	3,0	2,9	3,2	3,2	3,8	2,4
26/08/2021	4,9	4,5	4,0	4,1	3,7	3,9	3,3	3,6	2,0	-0,7	-1,9	-2,2	-2,5	0,0	1,7	0,9	1,3	1,9	3,1	3,6	3,9	4,3	5,1	5,2	2,4
27/08/2021	4,7	4,5	4,9	5,7	4,7	4,6	4,6	3,1	1,6	0,0	-1,4	-2,1													3,2
Total Geral	**4,3**	**4,3**	**4,2**	**4,5**	**4,3**	**4,3**	**4,3**	**3,4**	**1,0**	**-1,0**	**-1,9**	**-2,0**	**-2,1**	**0,0**	**2,2**	**0,9**	**0,2**	**0,7**	**1,9**	**3,1**	**3,3**	**3,6**	**3,8**	**4,0**	**2,2**

Figure 9 – Intensity and evolution of the climate heat island in P3 – Setor Bueno.
Source: Authors (2023).

Data	0:00	01:00	02:00	03:00	04:00	05:00	06:00	07:00	08:00	09:00	10:00	11:00	12:00	13:00	14:00	15:00	16:00	17:00	18:00	19:00	20:00	21:00	22:00	23:00	Total
18/06/2021																	2,6	3,3	4,1	3,5	4,2	5,1	5,3	5,2	4,2
19/06/2021	5,3	5,4	5,4	5,5	4,9	4,7	5,4	5,6	3,0	0,3	-1,0	-1,7	-1,2	0,6	3,7	3,7	2,3	2,7	3,3	3,6	3,8	4,4	4,9	5,4	3,3
20/06/2021	4,6	4,4	4,2	4,1	4,0	3,9	3,9	3,7	3,6	2,6	1,0	-0,2	-0,3	0,8	2,6	4,3	2,3	2,6	3,3	3,3	3,8	4,1	4,2	3,9	3,1
21/06/2021	4,0	4,1	4,1	4,7	5,1	4,9	5,1	4,9	4,4	1,9	-0,4	-1,3	-1,6	-0,4	3,0	2,7	1,1	2,3	3,7	4,1	4,3	5,0	5,2	4,8	3,2
22/06/2021	4,9	5,5	5,4	5,2	4,9	4,7	4,5	4,5	4,1	2,7	-0,4	-1,7	-1,1	-0,4	2,8	2,9	1,3	0,8	2,7	2,8	3,3	4,7	5,0	5,3	3,1
23/06/2021	5,6	5,4	5,4	5,9	5,6	5,5	5,3	5,2	3,8	1,4	-1,2	-2,2	-1,8	-0,6	2,8	2,4	0,3	1,7	3,5	4,1	4,3	4,6	5,1	5,0	3,2
24/06/2021	5,3	5,2	4,9	4,9	5,4	5,1	5,1	4,7	1,5	-0,2	-0,9	-1,1	-0,9	0,7	3,7	4,1	2,3	2,9	3,6	4,2	4,6	4,7	4,6	4,9	3,3
25/06/2021	5,6	5,7	5,6	5,6	4,9	4,9	4,9	4,5	3,7	1,3	-0,9	-1,7	-1,0	-0,1	2,0	3,0	0,3	2,2	3,7	3,7	4,1	4,3	4,4	4,1	3,1
26/06/2021	3,9	4,2	4,1	5,2	4,7	4,7	4,5	4,3	2,3	0,1	-0,9	-1,3	-1,0	0,0	2,8	2,5	0,2	-0,5	-1,1	-1,2	-1,9				1,7
Total	4,9	5,0	4,9	5,1	4,9	4,8	4,8	4,7	3,3	1,3	-0,6	-1,4	-1,1	0,1	2,9	3,2	1,4	2,0	3,0	3,1	3,5	4,6	4,8	4,8	3,1

Data	0:00	01:00	02:00	03:00	04:00	05:00	06:00	07:00	08:00	09:00	10:00	11:00	12:00	13:00	14:00	15:00	16:00	17:00	18:00	19:00	20:00	21:00	22:00	23:00	Total
19/08/2021																0,0	-0,4	-0,6	-0,5	-0,8	-1,3	-1,9	-2,5	-2,8	-1,2
20/08/2021	-3,1	-3,8	-4,3	-4,5	-4,8	-5,1	-5,2	-5,1	-4,5	-3,0	-1,7	-0,7	0,7	3,0	5,6	3,5	1,0	-0,5	-0,7	2,4	1,7	1,8	3,0	2,1	-0,9
21/08/2021	4,0	4,1	4,1	4,2	4,3	4,6	4,6	3,0	0,4	-1,8	-1,9	-1,5	-1,9	0,1	2,7	1,0	-0,4	-0,7	1,1	2,7	3,4	4,0	2,7	3,6	1,9
22/08/2021	4,0	4,0	4,3	4,5	4,2	3,0	3,1	1,8	-0,3	-1,4	-2,0	-2,0	-2,0	0,0	3,0	1,6	0,5	1,1	2,4	3,0	3,5	4,4	4,4	4,5	2,1
23/08/2021	3,9	4,1	4,2	4,9	5,3	5,5	5,1	3,7	1,1	-1,1	-2,1	-2,2	-2,1	0,3	2,0	1,0	-0,5	1,3	2,7	3,6	4,1	4,2	4,2	4,2	2,4
24/08/2021	4,1	4,0	3,4	3,2	2,9	4,0	4,5	3,9	1,3	-0,8	-2,0	-2,1	-2,3	-1,2	1,9	0,4	-0,8	0,6	2,3	3,3	3,4	3,5	4,0	4,7	1,9
25/08/2021	4,7	4,8	4,8	5,2	5,3	4,9	5,2	4,6	0,9	-1,1	-2,3	-2,2	-1,8	1,0	2,2	0,2	1,0	1,6	2,7	3,0	2,9	3,2	3,2	3,8	2,4
26/08/2021	4,9	4,5	4,0	4,1	3,7	3,9	3,3	3,6	2,0	-0,7	-1,9	-2,2	-2,5	0,0	1,7	0,9	1,3	1,9	3,1	3,6	3,9	4,3	5,1	5,2	2,4
27/08/2021	4,7	4,5	4,9	5,7	4,7	4,6	4,6	3,1	1,6	0,0	-1,4	-2,4	-2,7	-0,5	1,8	0,1	-0,7	-0,4	2,4	2,9	3,7	4,2	3,0	2,9	2,1
28/08/2021	3,0	3,0	2,6	1,3	1,1	3,0	3,4	3,2	0,8	-1,3	-1,8	-1,9	-1,8	0,1	1,3	-0,2	-0,8	-0,4	0,5	1,3	1,9	1,4	1,4	3,3	1,0
29/08/2021	2,8	3,5	4,4	4,7	4,2	4,4	3,7	1,8	0,0	-1,7	-1,9	-2,1	-2,0	-0,2	1,3	0,1	-0,6	-0,2	0,1	-0,2	0,1	0,5	0,4	0,6	1,0
30/08/2021	0,8	0,7	1,5	1,5	1,8	2,2	2,2	1,1	-0,1	-1,4	-2,3	-2,1	-2,0	-0,3	0,2	-0,7	0,4	0,1	0,1	0,1	0,1	0,2	0,1	0,0	0,2
31/08/2021	0,0	0,1	0,1	0,1	0,1	0,2	0,1	0,0	0,0	-0,3	-0,1	-0,1	-0,1	-0,1	-0,1	-0,1	0,1	0,7	0,7						0,0
Total	2,8	2,8	2,8	2,9	2,7	2,9	2,9	2,1	0,3	-1,2	-1,8	-1,8	-1,7	0,2	2,0	0,6	0,0	0,3	1,3	2,1	2,3	2,5	2,4	2,7	1,3

Data	0:00	01:00	02:00	03:00	04:00	05:00	06:00	07:00	08:00	09:00	10:00	11:00	12:00	13:00	14:00	15:00	16:00	17:00	18:00	19:00	20:00	21:00	22:00	23:00	Total
08/09/2021																-4,0	-1,4	0,0	1,8	2,9	3,3	3,8	4,1	4,3	1,8
09/09/2021	4,3	4,8	5,2	5,7	5,9	6,0	5,3	4,2	1,9	-0,8	-2,0	-2,8	-3,8	-4,1	-3,8	-3,2	-1,2	0,3	1,9	2,8	3,0	3,4	3,5	4,0	1,7
10/09/2021	5,0	4,7	3,1	1,5	1,9	2,6	2,1	1,9	0,0	-1,4	-1,3	-1,1	-2,0	-2,6	-2,7	-3,0	-1,2	0,0	1,0	2,1	1,3	0,3	0,7	0,7	0,6
11/09/2021	0,9	1,1	1,3	1,7	2,5	2,5	2,7	1,4	-0,7	-3,0	-3,1	-2,3	-3,7	-4,6	-4,2	-4,9	-1,5	0,2	1,8	2,1	2,9	3,6	3,1	4,4	0,2
12/09/2021	3,8	2,7	2,1	2,3	3,1	3,1	3,3	3,2	0,0	-3,2	-3,9	-3,5	-4,1	-3,2	-3,4	-4,0	-2,2	0,1	2,0	2,8	3,1	3,5	2,7	3,2	0,6
13/09/2021	3,4	3,9	4,4	4,3	4,2	5,0	6,1	5,1	0,6	-3,0	-5,5	-3,1	-3,4	-4,0	-2,8	-3,5	-1,3	0,2	2,8	3,6	4,0	3,5	3,8	4,5	1,4
14/09/2021	5,7	5,8	6,2	6,0	6,5	6,9	6,7	6,1	4,4	0,8	-1,4	-1,7	-3,1	-1,9	-0,5	-3,4	-0,7	0,6	2,1	2,7	3,0	4,2	4,2	4,1	2,6
15/09/2021	4,5	4,6	5,3	5,7	5,9	5,8	5,6	5,4	3,1	-0,4	-2,4	-3,7	-4,5	-3,6	-2,6	-4,3	-0,3	1,2	2,4	3,4	3,9	4,3	4,7	4,6	2,0
16/09/2021	5,3	5,6	6,0	5,8	6,3	7,0	7,3	6,2	2,6	-1,2	-2,2	-2,4	-3,8	-4,5	-4,3	0,6	2,7	0,2	-0,1	0,0					1,9
Total	4,1	4,2	4,2	4,1	4,5	4,8	4,9	4,2	1,5	-1,5	-2,7	-2,6	-3,5	-3,6	-3,0	-3,3	-0,8	0,3	1,7	2,7	3,0	3,3	3,3	3,7	1,4

Figure 7 – Intensity and evolution of the climate heat island in P1 – Setor Bueno.
Source: Authors (2023).

Data	0:00	01:00	02:00	03:00	04:00	05:00	06:00	07:00	08:00	09:00	10:00	11:00	12:00	13:00	14:00	15:00	16:00	17:00	18:00	19:00	20:00	21:00	22:00	23:00	Total
18/06/2021																			3,4	2,9	4,2	4,9	4,7	4,4	4,2
19/06/2021	4,4	4,7	4,7	4,7	4,3	4,9	5,3	5,4	3,8	4,7	6,1	5,2	5,0	4,2	3,8	2,7	4,2	3,8	3,9	3,2	3,4	4,1	4,5	4,7	4,4
20/06/2021	3,9	3,7	3,4	3,3	3,2	3,0	3,0	3,3	4,2	8,1	9,9	7,4	5,2	3,6	2,8	3,7	4,1	3,3	3,3	3,1	3,4	3,6	3,7	3,3	4,1
21/06/2021	3,2	3,1	3,1	3,8	4,2	3,9	4,4	4,4	4,7	7,1	8,5	5,7	4,8	3,7	2,8	1,7	4,3	3,6	3,9	4,0	3,9	4,6	4,8	4,4	4,3
22/06/2021	4,6	5,5	4,7	4,7	4,7	3,9	3,8	4,2	5,0	8,9	10,4	6,8	5,8	3,6	3,2	2,1	4,6	1,8	3,0	2,7	2,8	4,0	4,4	4,7	4,6
23/06/2021	4,8	4,7	5,0	5,0	4,9	4,7	4,5	5,1	3,9	4,6	5,9	5,5	4,6	3,3	2,9	1,4	3,2	2,8	3,7	3,9	4,0	4,4	5,1	4,9	4,3
24/06/2021	4,7	4,5	4,2	4,5	4,7	3,9	4,1	4,1	2,0	3,9	6,5	5,7	4,9	3,8	3,8	2,7	4,5	4,0	3,6	3,5	3,9	4,1	3,9	4,2	4,1
25/06/2021	5,1	5,3	4,9	4,6	4,2	4,1	4,0	4,0	4,0	5,3	6,4	6,0	5,8	3,6	2,9	2,8	3,4	3,1	4,0	3,7	3,5	3,6	3,6	3,3	4,2
26/06/2021	3,1	3,5	3,3	4,3	3,6	3,6	3,7	3,7	2,5	3,9	6,4	5,5	4,4	3,4	2,4	0,9	2,6								3,6
Total	**4,2**	**4,4**	**4,1**	**4,4**	**4,2**	**4,0**	**4,1**	**4,3**	**3,7**	**5,8**	**7,5**	**6,0**	**5,1**	**3,6**	**3,1**	**2,2**	**3,8**	**3,2**	**3,6**	**3,4**	**3,6**	**4,2**	**4,3**	**4,2**	**4,2**

Data	0:00	01:00	02:00	03:00	04:00	05:00	06:00	07:00	08:00	09:00	10:00	11:00	12:00	13:00	14:00	15:00	16:00	17:00	18:00	19:00	20:00	21:00	22:00	23:00	Total
19/08/2021																0,0	-0,1	-0,3	-0,6	-1,0	-1,8	-2,7	-3,1	-3,3	-1,4
20/08/2021	-3,9	-4,7	-5,2	-5,5	-5,7	-5,8	-6,0	-5,9	-4,4	-1,6	2,4	4,0	4,8	4,0	3,5	3,1	1,8	0,0	-0,5	2,3	1,3	1,2	2,3	1,4	-0,7
21/08/2021	3,3	3,3	3,5	3,5	3,8	3,8	4,1	2,7	0,8	-0,3	1,9	3,4	2,1	0,9	0,3	0,6	0,3	-0,1	1,3	2,6	3,0	3,6	2,1	2,8	2,2
22/08/2021	3,3	3,2	3,7	4,0	3,6	2,4	2,5	1,5	0,0	0,0	2,2	2,2	0,8	1,0	0,9	0,9	1,2	2,2	3,1	3,3	3,6	4,3	4,0	3,8	2,4
23/08/2021	3,2	3,4	3,5	4,2	4,6	4,8	4,7	3,5	1,7	0,6	2,6	3,3	3,7	1,2	1,4	1,7	1,0	2,5	3,5	4,0	4,3	4,3	4,0	3,9	3,1
24/08/2021	3,5	3,3	2,7	2,6	2,3	3,3	3,9	3,7	1,9	1,0	3,3	2,6	3,5	0,8	1,6	0,9	0,2	1,7	2,7	3,5	3,5	3,4	3,8	4,5	2,7
25/08/2021	4,3	4,2	4,3	4,8	4,8	4,5	4,7	4,3	1,2	0,8	3,1	3,6	3,6	2,1	1,8	1,3	2,9	3,1	3,5	3,6	3,3	3,4	3,1	3,6	3,3
26/08/2021	4,4	4,3	3,6	4,0	3,6	3,9	2,9	3,7	3,0	1,7	2,6	3,7	2,8	1,8	1,7	1,9	2,8	3,0	3,6	3,6	3,9	4,0	5,1	4,7	3,3
27/08/2021	4,1	3,9	4,3	5,1	3,8	3,7	3,7	2,4	1,8	1,4	2,7	3,0	2,7	0,9	1,1	0,7	0,7	0,5	2,9	3,2	3,7	3,8	2,4	2,5	2,7
28/08/2021	2,6	2,5	1,9	0,5	0,4	2,2	2,8	3,0	1,0	-0,2	0,8	3,0	2,2	0,8	0,4	0,4	0,0	0,0	0,4	1,0	1,3	0,7	0,7	2,5	1,3
29/08/2021	1,9	2,5	3,5	3,8	3,1	3,4	2,7	1,1	-0,2	-0,9	1,3	2,0	1,7	0,8	0,5	0,9	0,2	0,2	0,2	-0,4	-0,4	0,0	0,1	0,2	1,2
30/08/2021	0,4	0,4	1,1	1,3	1,2	1,7	1,6	0,9	0,3	0,4	2,1	3,1	2,6	0,6	0,1	-1,2	0,0	0,0	-0,1	-0,1	0,0	0,1	0,0	-0,1	0,7
31/08/2021	0,0	0,1	0,0	0,0	0,1	0,1	0,1	0,0	0,0	-0,2	-0,1	-0,1	-0,1	-0,2	-0,1	-0,2	-0,2	0,1	0,1						0,0
Total	2,2	2,2	2,2	2,3	2,1	2,3	2,3	1,7	0,6	0,2	2,1	2,8	2,5	1,2	1,1	0,9	0,8	1,0	1,6	2,1	2,1	2,2	2,0	2,2	1,8

Data	0:00	01:00	02:00	03:00	04:00	05:00	06:00	07:00	08:00	09:00	10:00	11:00	12:00	13:00	14:00	15:00	16:00	17:00	18:00	19:00	20:00	21:00	22:00	23:00	Total
07/09/2021																			0,6	0,6	-0,6	-0,4	0,1	0,1	0,1
08/09/2021	0,1	0,1	0,1	0,0	0,1	0,0	0,1	0,0	0,0	0,0	0,0	0,1	0,1	0,3	-3,1	-4,2	0,5	2,8	4,2	4,8	4,9	4,9	4,8	4,4	1,0
09/09/2021	4,2	4,8	5,0	5,2	5,0	5,1	4,4	4,2	2,8	1,4	2,4	1,4	0,7	0,4	1,0	0,7	2,0	2,9	3,9	4,0	4,0	4,0	4,1	4,5	3,2
10/09/2021	4,9	4,2	2,3	1,0	1,1	1,6	1,3	1,0	0,0	0,6	3,0	3,9	3,8	1,8	0,9	0,2	1,5	1,7	2,2	2,9	1,8	0,4	0,4	0,3	1,8
11/09/2021	0,4	0,5	0,6	0,8	1,5	1,8	1,8	1,1	-0,3	-0,4	2,4	3,1	1,7	1,2	0,2	-0,8	1,4	2,0	2,7	3,1	3,8	4,2	3,7	4,7	1,7
12/09/2021	4,0	2,5	1,8	1,9	2,5	2,7	2,8	3,0	0,5	-1,0	1,7	1,7	1,1	1,9	1,5	-0,2	0,6	2,1	3,5	3,9	4,0	4,4	3,4	3,8	2,2
13/09/2021	3,9	4,4	4,6	4,7	4,3	4,7	5,7	5,1	1,8	-0,2	1,9	2,1	2,8	1,1	1,1	-0,4	1,2	2,1	4,2	4,6	5,0	4,1	4,3	4,8	3,2
14/09/2021	5,6	5,2	5,4	5,2	5,4	5,2	5,2	4,9	3,8	2,2	2,7	2,2	1,0	2,5	3,3	-0,2	1,9	2,7	3,1	3,3	3,8	4,7	4,5	4,5	3,7
15/09/2021	4,7	4,4	4,8	4,7	5,0	4,7	4,4	4,5	3,7	2,3	2,1	1,9	1,6	1,6	1,5	-0,5	2,9	3,4	3,6	4,3	4,7	4,6	4,7	4,6	3,5
16/09/2021	4,9	4,9	5,4	4,7	5,0	5,5	5,9	5,3	3,0	1,0	1,8	3,2	2,9	1,6	0,9	4,1	5,4	0,4	0,0	0,2					3,4
Total	**3,6**	**3,4**	**3,3**	**3,1**	**3,3**	**3,5**	**3,5**	**3,2**	**1,7**	**0,6**	**2,0**	**2,2**	**1,7**	**1,4**	**0,8**	**-0,1**	**1,9**	**2,2**	**2,8**	**3,4**	**3,5**	**3,4**	**3,3**	**3,5**	**2,6**

Figure 8 – Intensity and evolution of the climate heat island in P2 – Setor Bueno.
Source: Authors (2023).

Data	0:00	01:00	02:00	03:00	04:00	05:00	06:00	07:00	08:00	09:00	10:00	11:00	12:00	13:00	14:00	15:00	16:00	17:00	18:00	19:00	20:00	21:00	22:00	23:00	Total
18/06/2021																		3,1	3,9	3,1	4,0	4,8	4,8	4,6	4,0
19/06/2021	4,6	4,9	4,7	4,6	4,2	4,8	5,1	5,2	2,8	0,0	-1,2	-1,7	-1,1	0,9	2,4	3,1	3,2	3,4	3,7	3,3	3,6	4,1	4,4	5,0	3,1
20/06/2021	4,7	4,6	4,5	4,4	4,2	3,9	4,0	4,0	3,6	2,8	1,2	-0,1	-0,2	0,5	2,0	3,3	2,5	2,8	3,4	3,4	3,8	4,1	3,9	3,4	3,1
21/06/2021	3,2	3,2	3,2	3,9	4,3	4,0	4,5	4,3	3,9	1,5	-0,5	-1,3	-1,7	-1,0	-0,1	1,0	1,0	2,2	3,3	3,8	3,9	4,6	4,9	4,9	2,5
22/06/2021	5,2	5,9	5,9	6,0	5,7	5,6	5,7	5,7	5,0	3,1	0,2	-1,5	-1,0	-1,1	-0,3	1,8	1,4	0,9	2,7	2,5	2,9	4,1	4,4	4,6	3,1
23/06/2021	4,9	4,9	5,3	5,3	5,1	5,0	5,3	5,3	3,1	0,9	-1,3	-2,2	-1,7	-0,9	0,0	1,7	0,6	1,7	3,4	3,8	3,9	4,3	4,9	4,8	2,8
24/06/2021	4,8	4,7	4,4	4,5	4,8	4,1	4,2	4,2	1,2	-0,4	-1,0	-1,4	-0,9	0,6	1,0	4,3	2,8	2,8	3,2	3,8	4,7	4,7	4,8	4,7	2,9
25/06/2021	5,4	5,4	5,2	4,9	4,4	4,1	4,2	4,1	3,3	1,2	-0,8	-1,5	-1,2	-0,6	0,3	2,4	0,6	2,2	3,6	3,6	3,6	3,7	3,8	3,7	2,7
26/06/2021	3,4	3,7	3,4	4,5	3,8	3,8	3,8	4,0	2,0	-0,2	-1,0	-1,4	-0,8	0,0	1,1	2,9	0,7	-0,4	-0,1	-0,1	0,1				1,6
Total	**4,5**	**4,6**	**4,6**	**4,7**	**4,5**	**4,4**	**4,6**	**4,6**	**3,1**	**1,1**	**-0,6**	**-1,4**	**-1,1**	**-0,2**	**0,8**	**2,5**	**1,6**	**2,0**	**3,0**	**3,0**	**3,5**	**4,3**	**4,5**	**4,4**	**2,8**

Data	0:00	01:00	02:00	03:00	04:00	05:00	06:00	07:00	08:00	09:00	10:00	11:00	12:00	13:00	14:00	15:00	16:00	17:00	18:00	19:00	20:00	21:00	22:00	23:00	Total
19/08/2021																0,1	0,1	0,0	-0,2	-0,6	-1,4	-2,4	-2,9	-3,0	-1,2
20/08/221	-3,5	-4,4	-4,8	-5,2	-5,5	-5,7	-5,7	-5,5	-4,5	-2,8	-1,3	-0,5	1,1	2,8	3,9	4,5	2,8	0,2	-0,2	2,6	1,6	1,5	2,6	1,7	-1,0
21/08/2021	3,4	3,6	3,6	3,8	4,0	4,1	4,3	2,9	0,3	-1,7	-1,8	-1,5	-1,6	-0,7	1,2	2,3	1,2	0,0	1,4	2,8	3,3	3,7	2,4	3,2	1,8
22/08/2021	3,6	3,6	4,0	4,2	3,9	2,5	2,5	1,5	-0,3	-1,5	-1,8	-1,9	-1,9	-0,5	1,4	2,5	2,2	1,4	2,1	2,6	3,5	4,3	4,1	4,1	1,9
23/08/2021	3,4	3,5	3,7	4,3	4,5	4,8	4,7	4,2	1,2	-1,1	-1,7	-1,8	-1,8	-0,5	0,4	2,3	0,9	2,1	3,1	3,7	4,3	4,3	4,3	4,2	2,4
24/08/2021	3,8	3,6	3,0	2,7	2,3	3,3	4,0	3,6	1,2	-0,8	-1,6	-1,9	-1,8	-1,1	0,6	0,1	-0,4	0,5	2,0	3,2	3,4	3,4	4,0	4,6	1,7
25/08/2021	4,6	4,3	4,1	4,7	4,8	4,4	4,8	4,5	0,9	-1,0	-2,0	-2,0	-1,4	0,4	1,1	1,2	2,1	1,9	2,5	3,0	3,1	3,1	3,1	3,8	2,3
26/08/2021	5,1	4,8	4,1	4,5	4,1	4,2	4,0	4,4	2,5	-0,3	-1,3	-1,6	-2,0	-0,1	0,3	2,6	2,2	2,4	3,8	4,3	4,6	4,7	5,2	4,9	2,8
27/08/2021	4,1	4,0	4,2	4,9	3,9	3,8	3,7	2,2	0,9	-0,3	-1,3	-2,3	-2,5	-0,9	0,8	3,2	0,7	-0,2	2,3	2,9	3,7	4,0	2,6	2,6	2,0
28/08/2021	2,8	2,8	2,1	0,7	0,5	2,4	3,0	3,0	0,7	-1,4	-1,9	-1,9	-1,5	-0,3	0,5	1,6	0,4	0,0	0,4	1,2	1,5	0,9	1,1	2,8	0,9
29/08/2021	2,2	2,9	3,8	4,0	3,3	3,7	3,1	1,3	-0,4	-2,1	-1,9	-2,0	-1,8	-0,4	0,6	0,4	-0,5	-0,4	-0,1	-0,8	-0,5	0,0	0,0	0,2	0,6
30/08/2021	0,4	0,4	1,1	1,3	1,3	1,7	1,8	0,8	-0,2	-1,2	-1,8	-1,7	-1,5	-0,5	0,2	0,9	1,4	0,8	-0,2	-1,0	-2,3	-2,7	-4,5	-4,2	-0,4
31/08/2021	-4,2	-4,3	-4,4	-4,8	-5,0	-5,3	-5,3	-5,2	-4,4	-2,9	-1,6	-0,7	0,9	2,3	3,2	4,0									-2,3
Total	**2,1**	**2,0**	**2,0**	**2,1**	**1,8**	**2,0**	**2,1**	**1,5**	**-0,2**	**-1,4**	**-1,7**	**-1,7**	**-1,3**	**0,0**	**1,2**	**2,0**	**1,1**	**0,7**	**1,4**	**2,0**	**2,1**	**2,1**	**1,8**	**2,1**	**1,1**

Data	0:00	01:00	02:00	03:00	04:00	05:00	06:00	07:00	08:00	09:00	10:00	11:00	12:00	13:00	14:00	15:00	16:00	17:00	18:00	19:00	20:00	21:00	22:00	23:00	Total
08/09/2021														0,2	-1,6	-3,8	-1,1	0,6	3,6	5,0	5,2	5,2	5,3	5,1	2,3
09/09/2021	4,7	5,2	5,6	5,7	5,6	6,0	5,2	4,1	2,3	0,0	-1,1	-2,6	-2,6	-1,0	0,5	0,2	1,4	2,5	3,8	4,3	4,4	4,5	4,7	5,1	2,8
10/09/2021	5,6	4,1	2,3	1,0	1,0	1,6	1,3	0,7	-0,8	-1,4	-1,6	-1,8	-1,7	-1,5	-1,0	-1,2	0,1	0,6	2,0	2,9	1,5	0,2	0,4	0,3	0,6
11/09/2021	0,3	0,3	0,6	0,9	1,7	2,1	2,0	0,9	-1,0	-2,1	-2,3	-2,9	-3,4	-1,8	-0,9	-1,0	-0,1	0,4	1,9	3,1	4,2	4,6	4,0	4,8	0,7
12/09/2021	3,9	2,7	2,1	2,1	2,8	2,8	3,1	2,9	-0,3	-2,8	-3,7	-3,7	-2,7	-0,3	0,6	0,9	-0,1	1,1	2,7	3,7	4,1	4,6	3,7	4,0	1,4
13/09/2021	4,1	4,3	4,7	4,5	4,1	4,8	5,8	5,0	1,3	-2,0	-2,8	-3,0	-2,2	-1,2	0,7	0,1	0,7	1,9	4,3	5,1	5,4	4,5	4,7	5,1	2,5
14/09/2021	6,2	6,1	6,0	5,9	6,3	6,4	5,8	5,3	3,7	0,7	-1,2	-2,2	-2,5	0,0	1,1	-0,3	1,3	2,4	3,4	3,8	4,3	4,9	4,8	4,9	3,2
15/09/2021	5,1	5,0	5,4	5,5	5,7	5,9	5,3	5,0	3,2	0,4	-1,3	-2,3	-1,6	-1,2	-0,1	-0,8	1,9	2,7	3,6	4,6	5,1	5,1	5,5	5,3	3,0
16/09/2021	5,6	6,0	6,1	5,9	6,5	7,4	7,7	6,3	2,5	-0,9	-1,8	-2,6	-3,0	-1,6	-0,6	3,9	4,6	0,2	0,1	0,1					2,7
Total	**4,4**	**4,2**	**4,1**	**3,9**	**4,2**	**4,6**	**4,5**	**3,8**	**1,4**	**-1,0**	**-2,0**	**-2,6**	**-2,5**	**-1,0**	**-0,1**	**-0,2**	**1,0**	**1,4**	**2,8**	**3,9**	**4,3**	**4,2**	**4,1**	**4,3**	**2,1**

Figure 10 – Intensity and evolution of the climate heat island in P4 – Setor Bueno.
Source: Authors (2023).

Point P3 showed the second highest UHI intensity among all periods. It is emphasized that, as mentioned earlier, the incomplete data caused by equipment problems prevent a more accurate reading of this point.

Finally, point P4 had the second lowest average UHI (1.9 ºC). Although the thermometer was situated on an avenue with heavy vehicle traffic, the extensive tree cover in the section caused the heat island phenomenon to be somewhat mitigated. Anyway, even with more intense tree cover, as it is the point farthest from the park, it was the location that presented the second highest maximum UHI, only behind the point located in the parking lot (P2).

However, when analyzing the data set, it is observed that points P1 and P4 recorded higher intensity of urban heat islands, recording 41% of events between 4 and 5°C, however these points were significant since they are points close to the park with tall buildings and tree-lined streets.

Point P4 and P2 recorded greater daytime heating. Point P1 and P3, less daytime heating. The explanation for the higher intensities of heat islands at points P4 and P2 can be found in Garland (2009) by stating that the differences in thermal behavior are distinguished by urban form, where wind plays a fundamental role, in addition to being points with greater vehicle and pedestrian traffic located in a parking lot in front of a shopping center – P2 and a double-lane avenue providing main access to the neighborhood – P4.

On average, the intensity of the nocturnal heat island was between 5 to 6°C compared to the rural point P5. Point P1 recorded greater nocturnal heating. The explanation for the higher intensities of heat islands at point 1 can be justified by the absence of ventilation, since the point faces a park but is located between the tallest buildings in the study area, between 60 to 90m. According to Akbari (2001), the building influences wind direction through shading. Point P3, the least nocturnal heating, as it is a point located in a ventilation corridor that provides access to the park, where there is an absence of barriers to wind circulation, which favors greater heat losses by convection.

Regarding the number of occurrences of urban heat islands, the classification of heat island intensity was demonstrated by Garcia and Alvares (2008), as presented in Table 4, where a higher number of occurrences was found, with 28% of cases for heat islands of weak magnitude and 21% of cases for heat islands with very strong magnitude.

The data obtained in the study corroborate the data from the IPCC Report (2019), where climate models project differences in regional climate characteristics between current days and global warming varying between 1.5°C and 2°C. Which, in turn, according to the research, would be heat islands of weak magnitude, corresponding to 28% of the episodes recorded in the study area.

The daytime points presented a very strong magnitude, where P1 (6 to 7°C), P2 (7 to 9°C), P3 (7 to 8°C), and P4 (9 to 10°C). The nocturnal points presented strong magnitude, P1 (5 to 6°C), P2, P3, and P4 (4 to 5°C). Thus, heat islands classified as strong and very strong occurred on 100% of the observed days.

Table 4 – Episodes of urban heat islands.

Variation (°C)	Magnitude	Number of occurrences	%
0°C - 2°C	weak	22	28%
2°C - 4°C	moderate	21	26%
4°C - 6°C	strong	20	25%
>6°C	very strong	17	21%
Total		80	100%

Source: Authors (2023).

3.2. Permeability of Horizontal Urban Surfaces

Little is known about how cities impact the daily evolution of urban heat islands and how they are distributed throughout the day (Moreira et al., 2019).

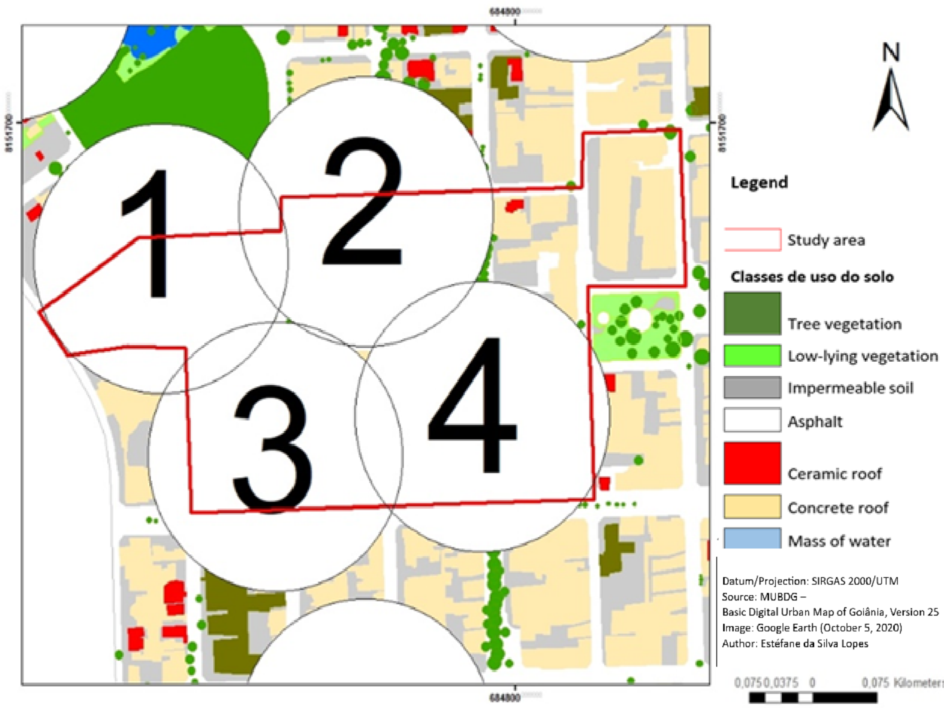

Source: Authors (2023).

Figure 11 presented the surroundings of Points 1, 2, 3, and 4. Figures 12 to 15 show the surroundings of each collection point, using Landsat 8 satellite images with the surface temperature of the point, as well as their respective permeabilities according to land use.

Figure 11 – Classification of Urban Points Location.
Source: Authors (2023).

Figure 11 presented the surroundings of Points 1, 2, 3, and 4. Figures 12 to 15 show the surroundings of each collection point, using Landsat 8 satellite images with the surface temperature of the point, as well as their respective permeabilities according to land use.

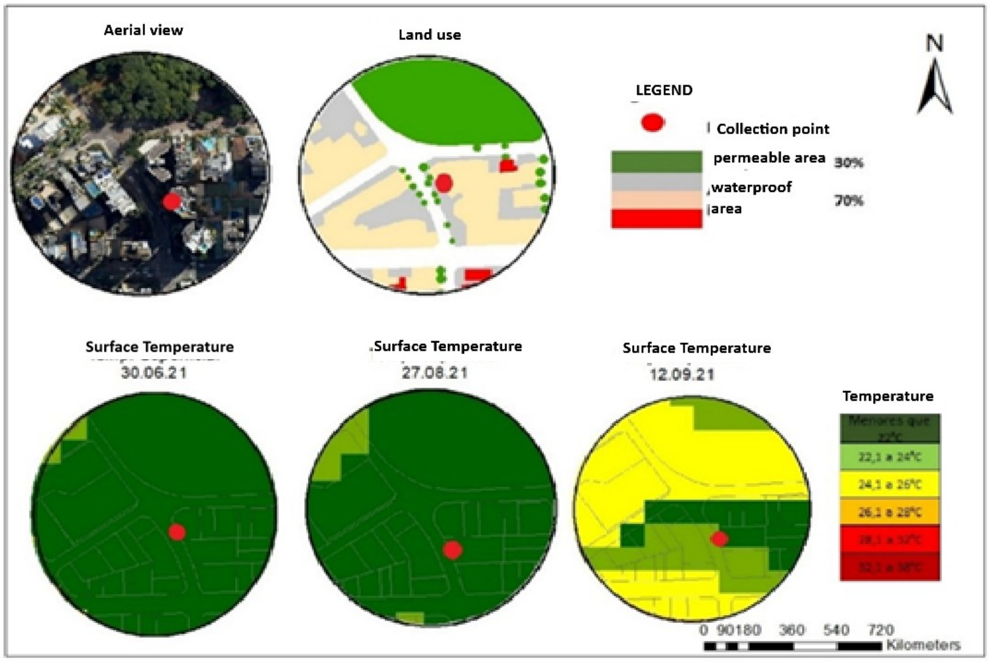

Figure 1 – Classification of permeability and surface temperature around Point 1.
Source: Authors (2023).

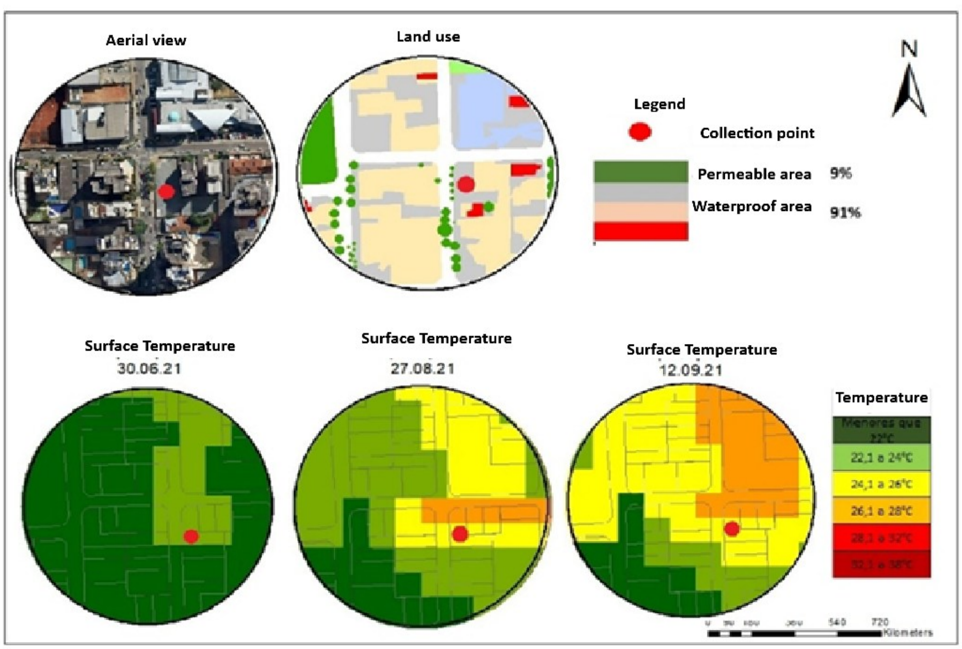

Figure 2 – Classification of permeability and surface temperature around Point 2.
Source: Authors (2023).

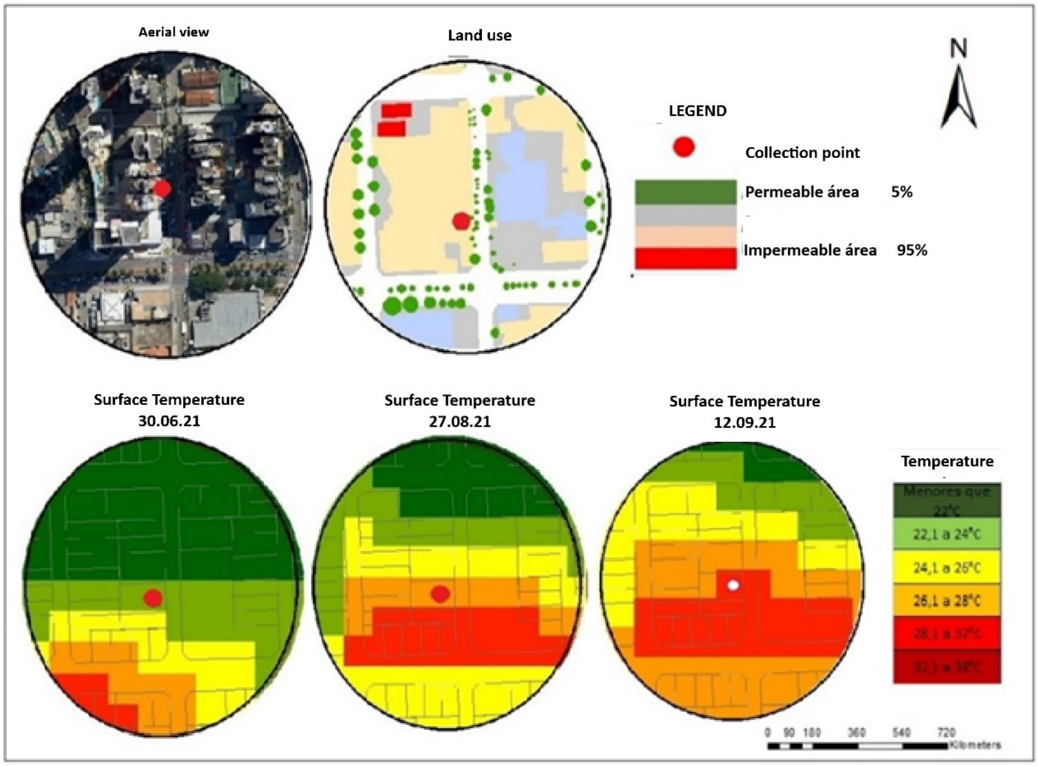

Figure 3 – Classification of permeability and surface temperature around Point 3.
Source: Authors (2023).

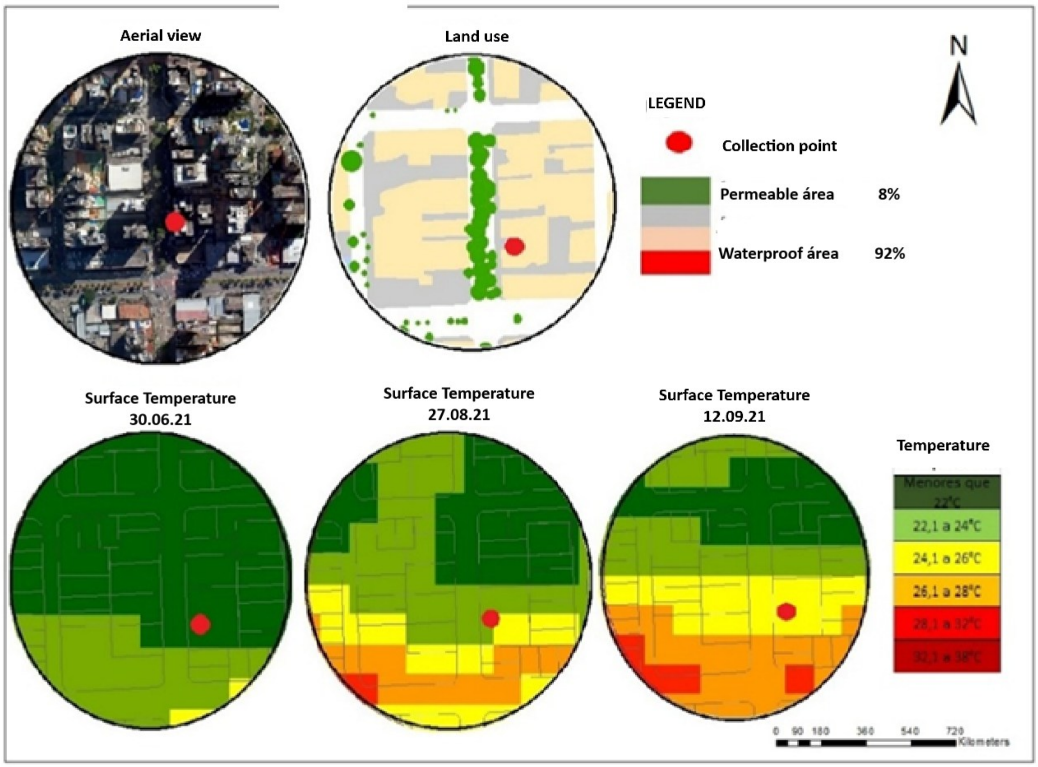

Figure 4 – Classification of permeability and surface temperature around Point 4.
Source: Authors (2023).

Considering the permeability of urban surfaces in the surroundings of each point, it is possible to see that Points 3 and 4 have only 5% and 8% of permeable surface respectively, being the lowest permeability values of all collected points, recording the highest surface temperature values relative to the months of June, August, and September 2021.

Point 1, however, has 30% of permeable area, being the location with the highest percentage of permeable surface and the lowest surface temperature relative to the months of June, August, and September 2021.

4. Final considerations

Among the three periods of urban climate: land use and occupation, thermo-physical properties of the soil, vegetation, presence of water bodies, urban geometry, ventilation, and permeability, the latter stands out for allowing water infiltration, which evaporates and cools the environment, while vegetation provides shading and reduces solar radiation reflection. Furthermore, the adequate arrangement of parks, squares, and green corridors facilitates wind circulation, dissipating pollutants and improving air quality; on the other hand, impermeable surfaces, such as asphalt and concrete, absorb and retain heat, raising local temperatures and creating hostile microclimates.

The lack of green areas and the predominance of impermeable surfaces exacerbate socio-environmental inequalities, mainly affecting vulnerable populations in densified neighborhoods. Strategies such as the creation of infiltration zones, the expansion of vegetated covers, and the planning of ventilation corridors should be incorporated into public policies and architectural projects, ensuring that vertical growth does not compromise thermal comfort and collective well-being. Examples such as the High Line in New York and the elevated parks in Seoul illustrate how the redevelopment of urban spaces can transform gray areas into green refuges, reducing heat islands and promoting climate resilience. Thus, permeability must be understood as an indispensable pillar for cities that aim to balance urban development and environmental sustainability.

The integration of permeable pavements, rain gardens, green roofs, and urban parks in verticalized neighborhoods not only mitigates the impacts of flash floods but also improves the microclimate, reducing heat islands and increasing biodiversity. Furthermore, permeable spaces promote real estate valuation and social well-being, creating areas for conviviality and leisure that humanize the built environment.

Public policies that encourage the retention and infiltration of rainwater - such as the review of land use coefficients and the requirement for green areas in new developments - are crucial for balanced urban development. The lack of permeability aggravates not only environmental problems but also social ones, mainly affecting peripheral communities, which are more susceptible to flooding. Therefore, rethinking land occupation in densified neighborhoods, prioritizing green infrastructure, is an indispensable step towards healthier, more resilient cities prepared for the challenges of the 21st century.

References

CHEN, Liang; YU, Bailang; YANG, Feng; et al. Intra-urban differences of mean radiant temperature in different urban settings in Shanghai and implications for heat stress under heat waves: A GIS-based approach. *Energy and Buildings*, v. 130, p. 829–842, 2016.

DENG, J. S. et al.Spatio-temporal dynamics and evolution of land use change and landscape pattern in response to rapid urbanization. *Landscape and Urban Planning*, v. 92, n. 3–4, p. 187–198, set. 2009.

DORIGON, L. P.; AMORIM, M. C. DE C. T. Spatial modeling of an urban Brazilian heat island in a tropical continental climate. *Urban Climate*, v. 28, p. 100461, jun. 2019.

DUARTE, D,; SERRA, G. Padrões de ocupação do solo e microclimas urbanos. *Techne*, São Paulo, n° 64, p.46-49, 2002.

EPA. United States Environmental Protection Agency. Heat Islands and Equity. Disponível em: https://www.epa.gov/heat-islands/heat-islands-and-equity.Acesso em junho de 2020.

HU, L.; BRUNSELL, N. A. The impact of temporal aggregation of land surface temperature data for surface urban heat island (SUHI) monitoring. *Remote Sensing of Environment*, v. 134, p. 162–174, jul. 2013.

IBGE - Instituto Brasileiro de Geografia e Estatística - cidades. Disponível em: www.cidades.ibge.gov.br/painel/painel.php?codmun=520870. Acesso em: 30jul. 2020.

IPING et al. (2019), Contribution of soil erosion to PAHs in surface water in China, v. 686, P.497-504, 10 October 2019.

LUAN, X.; Yu, Z.; ZHANG, Y.; WEI, S.; MIAO, X.; HUANG, Z.Y.X; TENG, S. N.; XU, C. Remote Sensing and Social Sensing Data Reveal Scale-Dependent and System-Specific Strengths of Urban Heat Island Determinants, *Remote Sensing*, v. 12, n. 3, p. 391, 2020.

NASCIMENTO, D. T. F. Emprego de técnicas de sensoriamento remoto e de geoprocessamento na análise multitemporal do fenômeno de ilhas de calor no município de Goiânia-GO (1986/2010). Dissertação (Mestrado) – Universidade Federal de Goiás, Instituto de Estudos Sócio-Ambientais, 2011

NAKATA-OSAKI, C. M.; SOUZA, L. C. L.; RODRIGUES, D. S. THIS – Tool for Heat Island Simulation: A GIS Extension Model to Calculate Urban Heat Island Intensity Based on Urban Geometry. Computers, *Environment and Urban Systems*, v. 67, p. 157–168, jan. 2018.

ONU. Divisão de População do Departamento de Assuntos Sociais Econômicos das Nações Unidas. Perspectivas mundiais de urbanização: A revisão de 2018; Edição Online; Nações Unidas: Nova York, NY, EUA, 2018.

OKE, T. R. The energetic basis of the urban heat island. Quarterly Journal of the Royal Meteorological Society, London, v. 108, n. 455, p. 1–24, 1982. Disponível em: <https://doi.org/10.1002/qj.49710845502>. Acesso em: 20 agosto. 2020.

OKE, T. R. Boundary layer climates. 2 nd ed. London and New York: Routledge. 1987.

PESAVENTO, Sandra Jatahy. Muito além do espaço: por uma história cultural dourbano. *Revista Estudos Históricos*, Rio de Janeiro, vol.8, n.16, 1995 (p.279-290)

RAJAGOPALAN, Priyadarsini; LIM, Kee Chuan; JAMEI, Elmira. Urban heat island and wind flow characteristics of a tropical city. *Solar Energy*, v. 107, p. 159–170, 2014.

SOUSA, S. B. DE; FERREIRA, L. G. Análise da temperatura de superfície em ambientes urbanos: um estudo por meio de sensoriamento remoto no município de Goiânia, Goiás (2002 – 2011). Confins, n. 15, 23 jun. 2012. Disponível em: <http://journals.openedition.org/confins/7631>. Acesso em: 13 maio 2019.

VALIN JR, M. O.; SANTOS, F. M. M. ; NOGUEIRA, M. C. J. A. ; DE MUSIS, C. R. ; NOGUEIRA, J. S. Utilização de Abrigos Termo-Higrométricos Alternativos. *Revista Caminhos de Geografia* (UFU), v. 17, p. 74-91, 2016.

WANG, Z F, The Relationship Between Land Use, Land Cover Change, And The Heat Island Effect In Xi'an City, China, *Applied Ecology and Environmental Research*, v. 17,